Strong cosmic censorship of the Euler-Heisenberg-dS black hole

Lu Chen[1,2] and Jia Tan[1,*]

[1]*School of Physical Science and Technology, Suzhou University of Science and Technology, Suzhou 215009, China*

[2]*School of Physics, Changchun Normal University, Changchun 130032, China*

(Received 12 March 2024; accepted 2 August 2024; published 4 September 2024)

The Euler-Heisenberg theory sheds light on the quantum electrodynamical vacuum corrections to the Maxwell-Lorentz theory. As a fundamental assumption to ensure spacetime causality, by examining the quasinormal modes of a massless neutral scalar field, we investigate the strong cosmic censorship (SCC) conjecture in the context of Euler-Heisenberg-de-Sitter black holes under the massless scalar perturbation. With the emergence of Euler-Heisenberg corrections, Euler-Heisenberg-dS black holes exhibit four horizons and two types of extremal conditions. The first type of extremal conditions, similar to the Reissner-Nordstrom-de Sitter (RNdS) spacetime, involves the coinciding Cauchy and event horizons, while the second type involves the innermost and Cauchy horizons coinciding. Through numerical calculations, we find that SCC is violated not only near the commonly observed first-type extremal solutions but also in the vicinity of second-type extremal black holes. This marks the first instance of SCC violation in another region besides the vicinity of first-type extremal black holes within the classical framework. Additionally, we observe that the validation region of charge ratio shrinks as the reduced Euler-Heisenberg parameter α/M^2 increases, and beyond a critical value of α/M^2, all black hole solutions violate SCC. These findings suggest a greater likelihood of SCC violation with higher reduced Euler-Heisenberg parameter values. Furthermore, when α/M^2 is sufficiently large, not only is the Christodoulou version of SCC violated but also the C^2 version. This marks the first instance of C^2 version SCC violation found under massless scalar field perturbations. Finally, we extend our research to cases where the scalar field nonminimally couples to electromagnetic invariants and find that, similar to the RNdS case, when the coupling constant b is sufficiently large, the SCC can also be restored in Euler-Heisenberg-dS black holes.

DOI: 10.1103/PhysRevD.110.064003

I. INTRODUCTION

Predictability is considered a fundamental principle in classical physics. To ensure the predictability of spacetime, Penrose proposed the strong cosmic censorship (SCC) conjecture [1]. This conjecture requires that spacetime be globally hyperbolic, enabling us to predict the evolution of the Universe by specifying reasonable initial data on a spacelike hypersurface, also known as a Cauchy hypersurface. The establishment of the SCC imposes two key restrictions on spacetime. Firstly, it demands the absence of naked singularities, as their presence would severely disrupt the causal structure of spacetime. This condition is commonly referred to as the weak cosmic censorship (WCC) conjecture. Secondly, it requires the absence of Cauchy horizons or that Cauchy horizons are nonextendible [2,3]. If a theory violates the SCC, the physical processes described by that theory become unpredictable. In a recent development, Sorce and Wald proposed a new gedanken experiment utilizing the Noether charge method [4]. This experiment showed the validation of WCC within Kerr-Newman black holes under second-order perturbation approximations. Subsequent discussions extended to various gravity and black hole models [5–17], mostly affirming black hole integrity and preventing the existence of naked singularities in spacetime.

Recent research has focused on different versions of the SCC, particularly exploring the stability of black hole Cauchy horizons. Christodoulou proposed a more precise formulation [18], emphasizing that when the Einstein field equations satisfy specific physical requirements, the maximal Cauchy development is nonextendible. Depending on the extendibility of spacetime at the Cauchy horizon, this conjecture can be categorized into several versions, with the strictest being the C^0 version, which demands the metric cannot be continuously extended at the Cauchy horizon. The C^2 version relaxes this condition to C^2 nonextendibility. Additionally, the Christodoulou version requires that weak solutions of the Einstein equations cannot be extended beyond the Cauchy horizon.

An important research direction for the Christodoulou version of the SCC is the linear perturbation of matter fields. In some cases, such as Reissner-Nordstrom (RN)

*Contact author: jiatansust@163.com

and Kerr black holes, this conjecture holds due to the influence of the blueshift effect [19–22]. However, when considering asymptotically de Sitter (dS) situations, the weakening of the blueshift effect may lead to the conjecture no longer holding, requiring further study to validate its effectiveness [23]. In dS spacetime, perturbations with varying spin properties demonstrate quasinormal modes (QNMs) decaying exponentially quicker outside the event horizon, prompting a redshift effect to offset the blueshift effect [24–29].

Research by Cardoso *et al.* found that for massless scalar field perturbations in RNdS black holes, the Christodoulou version of the SCC is violated in the near-extremal region [30]. Other studies suggest that violations may also occur with charged scalar fields and Dirac fields [31,32]. Similar situations have been observed in some modified gravity and black-hole models [33–50]. Through research on classical perturbations of non-minimally coupled scalar fields in Reissner-Nordstrom-de Sitter (RNdS) black holes, it was found that the conjecture can be restored within certain parameter ranges [51–53]. Additionally, research by Hollands *et al.* [54] indicates that considering semiclassical quantum fields in spacetime leads to important insights into the SCC in RNdS black holes, revealing that nonsingular initial quantum field data (known as Hadamard states) always lead to the appearance of singular Cauchy horizons, thereby restoring the effectiveness of the conjecture.

Nonlinear electrodynamics (NLED), a crucial branch of electromagnetic theory, explores the intricate nonlinear interactions between electromagnetic fields and charges. Originating with Mie's pioneering model of nonlinear electrodynamics in 1912 [55], and extending to the illustrious Born-Infeld nonlinear electrodynamics theory introduced by Born and Infeld in the 1930s [56], this field has seen continuous advancement. With the emergence of string theory, Born-Infeld type electrodynamics is recognized as an effective theory within string theory, sparking a resurgence of interest in nonlinear electrodynamics [57–60]. Moreover, solutions to the Born-Infeld equations have garnered considerable attention, as they are interpreted as states of D-branes, providing vital insights into the Universe's structural framework [61].

The Euler-Heisenberg black hole is a charged black hole solution within the Einstein-Euler-Heisenberg framework [62], arising from the coupling of nonlinear electrodynamics with Einstein gravity. The Euler-Heisenberg theory [63,64], conceived in 1936, elucidates the quantum electrodynamical vacuum corrections to the Maxwell-Lorentz theory. This theory has been firmly established and is presently undergoing experimental scrutiny to ascertain the nonlinear electromagnetic effects engendered under critical field or Schwinger field, characterized by an electric field intensity of 10^{18} V/m (or magnetic field of 10^9 T) [65].

As a fundamental assumption ensuring the causality of spacetime, a natural question arises: does the Einstein-Euler-Heisenberg theory satisfy the SCC? Therefore, our paper aims to investigate this question by considering perturbations of massless scalar fields in the context of Euler-Heisenberg-dS (EHdS) black holes and evaluating the stability of the Cauchy horizon under such perturbations. The subsequent sections of the paper proceed as follows: Sec. II provides a brief overview of the Einstein-Euler-Heisenberg theory and the spacetime geometry of the EHdS black hole, followed by Sec. III, where we analyze the massless scalar field and assess the implications for the validity of SCC. Section IV employs detailed numerical methods to evaluate the QNMs and analyze potential violations of SCC. Finally, the paper concludes by synthesizing the research findings.

II. EULER-HEISENBERG-DS BLACK HOLES

In this paper, we consider the Einstein-Euler-Heisenberg theory in which the general relativity with a cosmological constant is coupled to NLED. The action of the theory is given by [63,66,67]

$$S=\frac{1}{4\pi}\int_{\mathcal{M}} d^4x\sqrt{-g}\left[\frac{1}{4}(R-2\Lambda)-\mathcal{L}(\mathcal{F},\mathcal{G})\right], \quad (1)$$

with

$$\mathcal{L}(\mathcal{F},\mathcal{G})=-F+\frac{\alpha}{2}\mathcal{F}^2+\frac{7\alpha}{8}\mathcal{G}^2, \quad (2)$$

in which g_{ab} is the metric of the spacetime $\mathcal{M}$, R is the Ricci scalar, Λ is the cosmological constant, and

$$\mathcal{F}=\frac{1}{4}F_{\mu\nu}F^{\mu\nu} \quad \text{and} \quad \mathcal{G}=\frac{1}{4}F_{\mu\nu}{}^{*}F^{\mu\nu} \quad (3)$$

are two electromagnetic invariants with the electromagnetic strength $\boldsymbol{F}=\mathrm{d}\boldsymbol{A}$ and ${}^{*}F^{ab}=\epsilon_{abcd}F^{cd}/(2\sqrt{-g})$ its dual. When $\alpha=0$, the theory becomes Maxwell electrodynamics $\mathcal{L}(\mathcal{F},\mathcal{G})=-\mathcal{F}$. Here, α is the Euler-Heisenberg parameter, which regulates the intensity of the NLED contribution. It is not a free parameter and is given by $\alpha=8\alpha_0^2/45m_e^4\geq 0$ in physically relevant contexts, where m_e is the electron mass and α_0 is the fine structure constant.

By varying the action (1), the field equations can be obtained, and they are given by

$$\begin{aligned}\nabla_a P^{ab}&=0,\\ G_{ab}+\Lambda g_{ab}&=8\pi T^{\mathrm{EM}}_{ab},\end{aligned} \quad (4)$$

with Einstein tensor $G_{ab}=R_{ab}-(1/2)Rg_{ab}$ and

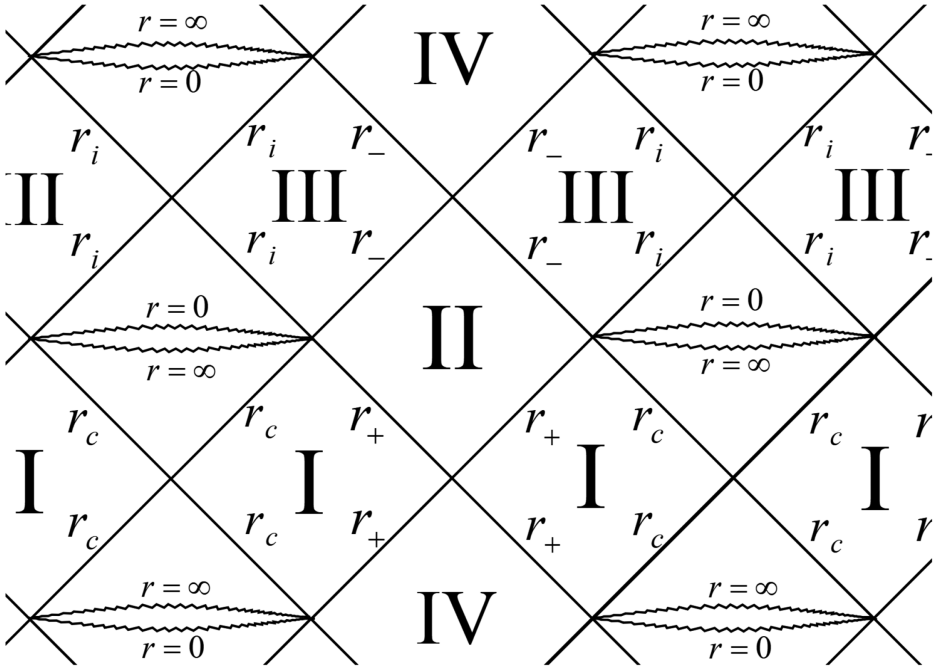

FIG. 1. The Penrose diagram of the EHdS black hole with three inner horizons, where region I is the physical region located at $r_+ < r < r_c$, regions II and III are the interior regions of the black hole located at $r_- < r < r_+$ and $r_i < r < r_-$ respectively, and region IV presents the white hole.

$$P_{ab} = (1-\alpha\mathcal{F})F_{ab} - {}^*F_{ab}\frac{7\alpha}{4}\mathcal{G},$$
$$T^{\mathrm{EM}}_{ab} = \frac{1}{4\pi}\left[(1-\alpha\mathcal{P})P_a{}^c P_{bc} + g_{ab}\left(\mathcal{P} - \frac{3}{2}\alpha\mathcal{P}^2 - \frac{7\alpha}{8}\mathcal{O}^2\right)\right]. \tag{5}$$

Here we denoted

$$\mathcal{P} = -\frac{1}{4}P_{ab}P^{ab} \quad \text{and} \quad \mathcal{O} = -\frac{1}{4}P_{ab}{}^*P^{ab}. \tag{6}$$

The static and spherically symmetric solution with an electric charge is given by [62,68]

$$ds^2 = -f(r)dt^2 + \frac{1}{f(r)}dr^2 + r^2(d\theta^2 + \sin^2\theta d\phi^2),$$
$$P_{\mu\nu} = \frac{Q}{r^2}\delta^0_{[\mu}\delta^1_{\nu]}; \tag{7}$$

with blackening factor

$$f(r) = 1 - \frac{2M}{r} + \frac{Q^2}{r^2} - \frac{\Lambda r^2}{3} - \frac{\alpha Q^4}{20r^6}, \tag{8}$$

where M and Q represent the mass and electric charge of the black hole, respectively. When $\alpha = 0$, the black hole solution reverts to the RNdS solution. Owing to $\alpha > 0$ Euler-Heisenberg theory, the last term in the blackening factor enhances the gravitational attraction compared to the metric function of RNdS black holes, regardless of the sign of the charge Q.

From the expression of $f(r)$ and considering that the Euler-Heisenberg parameter α is positive, it is easy to see that as $r \to 0$, $f(r) \to -\infty$, and as $r \to \infty$, $f(r) \to -\infty$. Therefore, the number of horizons for the Euler-Heisenberg-dS black hole must be even, and when the number of horizons is odd, there must be two horizons overlapping.

As our paper mainly discusses the stability of the Cauchy horizon in dS spacetime, it is necessary for the black hole to have both cosmological and Cauchy horizons. In other words, we consider a black hole characterized by four distinct horizons: the innermost horizon r_i, the Cauchy horizon r_-, the event horizon r_+, and the cosmological horizon r_c, satisfying the sequence $r_i < r_- < r_+ < r_c$. The Penrose diagram of the EHdS black hole is shown in Fig. 1. The surface gravity associated with each horizon is determined by

$$\kappa_j = \frac{1}{2}|f'(r_j)|, \tag{9}$$

where j ranges over $\{i, -, +, c\}$. Unlike the RNdS case, there are two critical conditions for the existence of the Cauchy horizon at this time. One is to make the event horizon and the Cauchy horizon coincide by increasing the black hole charge, which we call the first-type extremal black hole, as shown on the left side of Fig. 2; the other is to make the innermost horizon and the Cauchy horizon coincide by decreasing the charge, which we call the

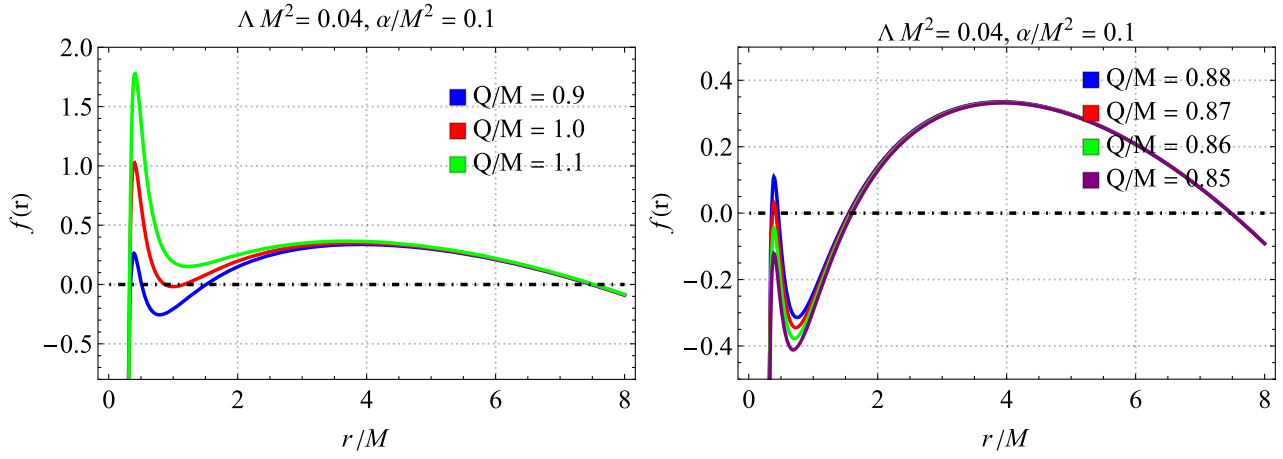

FIG. 2. The blackening factor $f(r)$ as a function of radial coordinate r across various parameters in the EHdS black hole.

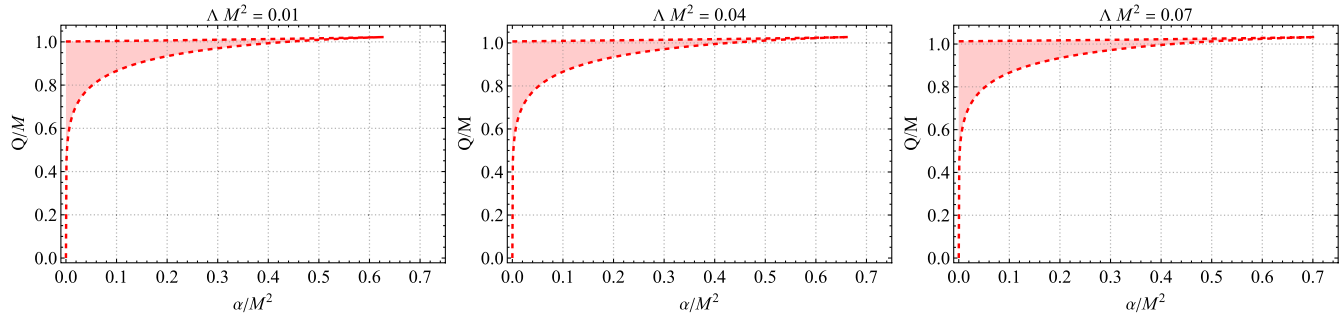

FIG. 3. The shaded regions in the $\alpha/M^2 - Q/M$ diagram indicate the parameter spaces where fourth horizons exist, corresponding to $\Lambda M^2 = 0.01$, 0.04, and 0.07.

second-type extremal black hole, as shown on the right side of Fig. 2.

In Fig. 3, we draw the parameter ranges of black hole solutions with both Cauchy and cosmological horizons in the $\alpha/M^2 - Q/M$ diagram for $\Lambda M^2 = 0.01, 0.04$, and 0.07. There are two boundaries, with the upper boundary given by the first-type extremal black hole and the lower boundary given by the second-type extremal black hole. It is evident from the figure that when α is not zero, such EHdS solutions not only have a maximum value of charge $Q_{\max}$ but also have a minimum value of charge $Q_{\min}$.

Through discussions by Cardoso *et al.* on RNdS black holes [30], it is known that the region of violation of the Christodoulou version of SCC mainly lies near extremal black holes, corresponding to our first-type extremal black holes in EHdS solutions. A similar question arises: will the SCC also be violated when approaching the second-type extremal black hole? This constitutes the primary focus of discussion in the subsequent sections.

III. MASSLESS SCALAR FIELD PERTURBATION AND STRONG COSMIC CENSORSHIP

Next, we consider the minimally coupled massless scalar field perturbation in EHdS black holes. In this scenario, the Einstein equations transform into

$$G_{ab} - \frac{1}{2}Rg_{ab} = T^{\mathrm{EM}}_{ab} + T^{\mathrm{SC}}_{ab}, \tag{10}$$

where

$$T^{\mathrm{SC}}_{ab} = 2\nabla_a\Psi\nabla_b\Psi - g_{ab}\nabla_c\Psi\nabla^c\Psi \tag{11}$$

represents the energy-momentum tensor of the scalar field. Furthermore, the equation of motion for the scalar field is given by

$$\nabla_a\nabla^a\Psi = 0. \tag{12}$$

Subsequently, we examine the stability of the Cauchy horizon under the aforementioned perturbations. For the Christodoulou version of SCC, it demands that our spacetime solution cannot be extended as a weak solution near the Cauchy horizon. If the gravitational field $g_{\mu\nu}$, electromagnetic field A_μ, and scalar field Ψ can be extended as weak solutions beyond the Cauchy horizon, then for any smooth and compactly supported test function Φ, it satisfies [30,46,51,52]

$$\int_{\mathcal{V}} d^4x\sqrt{-g}(G_{\mu\nu}-\Lambda g_{\mu\nu}-8\pi T^{\mathrm{EM}}_{\mu\nu}-T^{\mathrm{SC}}_{\mu\nu})\Phi=0. \quad (13)$$

The conditions outlined above require that each integral term in the equation is integrable. Considering the first two terms, given that the Riemann curvature is composed of Christoffel symbols Γ and their derivatives, we can deduce that

$$\int_{\mathcal{V}} d^4x\sqrt{-g}(G_{\mu\nu}-\Lambda g_{\mu\nu})\Phi \sim \int_{\mathcal{V}} d^4x\sqrt{-g}(\partial\Phi)\Gamma+\int_{\mathcal{V}} d^4x\sqrt{-g}\Gamma^2\Phi. \quad (14)$$

Hence, ensuring the finiteness of these integrals near the Cauchy horizon necessitates that Γ belongs to the space of locally square-integrable functions, i.e., $\Gamma\in L^2_{\mathrm{loc}}$.

For the electromagnetic field part, to ensure the weak solution extends beyond the Cauchy horizon, we require $T^{\mathrm{EM}}_{\mu\nu}$ to be integrable near the Cauchy horizon, i.e., $T^{\mathrm{EM}}_{\mu\nu}\in L^1_{\mathrm{loc}}$. This condition imposes certain constraints on A_μ.

Concerning the scalar field part, we have

$$\int_{\mathcal{V}} d^4x\sqrt{-g}T^{\mathrm{SC}}_{\mu\nu}\Phi\sim\int_{\mathcal{V}} d^4x\sqrt{-g}(\partial\Psi)^2\Phi. \quad (15)$$

The boundedness of this integral leads to the requirement that the derivative of the scalar field Ψ must be locally square integrable, signifying $\Psi\in H^1_{\mathrm{loc}}$.

In summary, to extend the weak solution beyond the Cauchy horizon, we need to ensure that the conditions $\Gamma\in L^2_{\mathrm{loc}}$, $T^{\mathrm{EM}}_{\mu\nu}\in L^1_{\mathrm{loc}}$, and $\Psi\in H^1_{\mathrm{loc}}$ are all satisfied. When considering scalar field perturbations, the extension of the weak solution beyond the Cauchy horizon requires that all existing scalar fields fulfill $\Psi\in H^1_{\mathrm{loc}}$.

Moving forward, we delve into the decomposition of the scalar field under spherical symmetry and time translational invariance

$$\Psi(t,r,\theta,\phi)=\sum_{l,m} e^{-i\omega t}Y_{lm}(\theta,\phi)\frac{\psi(r)}{r}, \quad (16)$$

where $Y_{lm}(\theta,\phi)$ denotes the spherical harmonics. Then, we have

$$\frac{d^2\psi(r)}{dr_*^2}+[\omega^2-V(r)]\psi(r)=0 \quad (17)$$

with the tortoise coordinate

$$r_*=\int_{r_0}^{r}\frac{dr}{f(r)} \quad (18)$$

and the effective potential

$$V(r)=\frac{f(r)}{r^2}\left[l(l+1)+\frac{2M}{r}-\frac{2Q^2}{r^2}-\frac{2\Lambda r^2}{3}+\frac{3\alpha Q^4}{10r^6}\right]. \quad (19)$$

Here we set $r_+<r_0<r_c$.

The solutions satisfying the boundary conditions

$$\psi\sim e^{-i\omega r_*},\qquad r\to r_+\quad (r_*\to-\infty),$$
$$\psi\sim e^{i\omega r_*},\qquad r\to r_c\quad (r_*\to\infty) \quad (20)$$

are referred to as QNMs. These boundary conditions dictate that the scalar field exhibits ingoing waves near the event horizon and outgoing waves near the cosmological horizon, conforming to scenarios where the initial values of the matter field are confined within a finite region between the event and cosmological horizons [69]. Under these boundary conditions, the behavior of QNMs near the Cauchy horizon is described by [51,52]

$$\Psi\sim e^{i\frac{\omega}{\kappa_-}\ln|r-r_-|}\propto|r-r_-|^\beta, \quad (21)$$

where

$$\beta\equiv-\frac{\mathrm{Im}(\omega)}{\kappa_-}. \quad (22)$$

For the weak solution to extend beyond the Cauchy horizon, it requires the local square integrability of the derivative of the scalar field (i.e., $\Psi\in H^1_{\mathrm{loc}}$), necessitating

$$\beta>1/2. \quad (23)$$

Typically, the initial values of our matter field are set within the physical spacetime region, i.e., between r_+ and r_c [69]. Under these circumstances, the scalar field must adhere to specific boundary conditions that ensure only ingoing waves near the event horizon and outgoing waves near the cosmological horizon. These conditions are precisely defined as

$$\psi\sim e^{-i\omega r_*},\qquad r\to r_+\quad (r_*\to-\infty),$$
$$\psi\sim e^{i\omega r_*},\qquad r\to r_c\quad (r_*\to\infty). \quad (24)$$

To satisfy these boundary conditions, certain restrictions on the scalar field frequency ω are necessary. The solution Ψ obtained under these conditions is known as the QNM, and the corresponding ω is referred to as the QNM frequency. We will next explore the relationship between these QNM frequencies and the validity of the SCC in de Sitter-like spacetimes.

The asymptotic solution near the Cauchy horizon reveals that the key aspect for regularity is [51,52]

$$\Psi\sim e^{i\frac{\omega}{\kappa_-}\ln|r-r_-|}\propto|r-r_-|^\beta \quad (25)$$

with

$$\beta \equiv -\frac{\mathrm{Im}(\omega)}{\kappa_-}. \tag{26}$$

From the preceding discussion, it follows that for the weak solution of the scalar field to extend beyond the Cauchy horizon, the derivative of the scalar field must be locally square integrable, i.e., $\Psi \in H^1_{\mathrm{loc}}$, which implies

$$\beta > 1/2. \tag{27}$$

Therefore, to uphold the SCC under scalar field perturbations, it is necessary for at least one QNM to exist such that the Cauchy horizon becomes inextendible within the realm of weak solutions under these perturbations. In other words, the lowest-lying mode must satisfy

$$\beta \leq 1/2. \tag{28}$$

Finally, we investigate the C^2 version of the SCC, which requires that the scalar field $\Psi(r)$ cannot be extended to be C^2 beyond the Cauchy horizon. From Eq. (25), it is clear that this condition necessitates the lowest-lying QNMs to satisfy

$$\beta \leq 1. \tag{29}$$

IV. NUMERICAL METHODS AND RESULTS

A. Numerical methods

Taking into account the boundary conditions (24) for QNMs, we introduce a new variable $y(r)$ as follows:

$$\psi(r) = (x+1)^{\frac{i\omega}{2\kappa_+}}(x-1)^{-\frac{i\omega}{2\kappa_c}} y(x), \tag{30}$$

where

$$r = \frac{r_c - r_+}{2} x + \frac{r_c + r_+}{2}. \tag{31}$$

Under this variable, the field equation (17) becomes a regular form within $[-1, 1]$, and $y(x)$ is analytic throughout the interval. Hence, we can employ the pseudospectral method [70,71] to solve it. Expanding $y(x)$ using nth-order basis functions $C_i(x)$, i.e., $y(x) = \sum_{i=0}^{n} z_i C_i(x)$, and evaluating the regularized equation at $n+1$ grid points x_j, we can transform it into a matrix equation, thereby converting the QNM frequency ω into the eigenvalues of this matrix. Then, by solving for the eigenvalues of the matrix, we can obtain the QNM frequencies.

In addition to the pseudospectral method mentioned above, we will also employ the direct integration method [72,73] to validate our numerical results, ensuring computational accuracy. Furthermore, due to challenges in computing for large angular momenta (large l), we will utilize the WKB approximation [74] to compute the QNMs in the large l limit (photosphere mode).

For the direct integration method, given a specific ω, we can obtain the series solutions of $y(x)$ at $x = \pm 1$ using the regularized equation. Then, using these solutions as boundary conditions, we can individually compute the solutions within the intervals $(-1, 0]$ and $[0, 1)$ using *Mathematica*. Finally, to ensure the smoothness of the solutions at $x = 0$, we determine acceptable frequencies ω.

B. Numerical results

In Tables I–III, we conducted computations of the lowest-lying QNMs, characterized by $\beta = -\mathrm{Im}(\omega)/\kappa_-$, using the pseudospectral method, direct integration method, and the WKB approximation in the large l limit, respectively. These calculations were performed for massless scalar fields in Euler-Heisenberg-dS black holes, considering different charge ratios $\chi = (Q - Q_{\mathrm{min}})/(Q_{\mathrm{max}} - Q_{\mathrm{min}}) = 0.1$ and various values of l, while keeping parameters $\Lambda M^2 = 0.01$ and α/M^2 fixed. Our numerical analyses affirm the reliability of these methods in determining the lowest-lying QNMs in EHdS black holes.

Figures 4 and 5 illustrate the interrelation between the lowest-lying QNMs' β and the extremal charge ratio $\chi = (Q - Q_{\mathrm{min}})/(Q_{\mathrm{max}} - Q_{\mathrm{min}})$, under specific values of ΛM^2 and the Euler-Heisenberg parameter α/M^2. For $\chi = 1$, representing first-type extremal black holes where the event and Cauchy horizons coincide $(r_+ = r_-)$, and $\chi = 0$, representing second-type extremal black holes where the innermost and Cauchy horizons coincide $(r_i = r_-)$, the plots consistently show that as χ approaches 1, indicative of nearly extremal black holes of the first type, the corresponding lowest-lying QNMs' β values remain consistently below $1/2$, thereby violating the Christodoulou version of the SCC. Moreover, unlike scenarios involving RNdS black holes or other

TABLE I. Computing the lowest-lying QNMs $\beta = -\mathrm{Im}(\omega)/\kappa_-$ based on various numerical methods for various l values, with $\Lambda M^2 = 0.01$, $\alpha/M^2 = 0.1$, and the charge ratio $\chi = (Q - Q_{\mathrm{min}})/(Q_{\mathrm{max}} - Q_{\mathrm{min}}) = 0.9$.

	$l=0$	$l=1$	$l=2$	$l=10$	$l=20$
Pseudospectral method	0.418505	0.252573	0.385369	0.384982	0.383254
Direct integration method	0.418545	0.253545	0.386524	0.388546	0.387545
WKB approximation				0.383374	0.383218

TABLE II. Computing the lowest-lying QNMs $\beta = -\mathrm{Im}(\omega)/\kappa_-$ based on various numerical methods for various l values, with $\Lambda M^2 = 0.01$, $\alpha/M^2 = 0.1$, and the charge ratio $\chi = (Q - Q_{\min})/(Q_{\max} - Q_{\min}) = 0.5$.

	$l = 0$	$l = 1$	$l = 2$	$l = 10$	$l = 20$
Pseudospectral method	0.122511	0.070449	0.113052	0.112366	0.112632
Direct integration method	0.122524	0.072421	0.112821	0.113230	0.112524
WKB approximation				0.112357	0.112333

TABLE III. Computing the lowest-lying QNMs $\beta = -\mathrm{Im}(\omega)/\kappa_-$ based on various numerical methods for various l values, with $\Lambda M^2 = 0.01$, $\alpha/M^2 = 0.1$, and the charge ratio $\chi = (Q - Q_{\min})/(Q_{\max} - Q_{\min}) = 0.1$.

	$l = 0$	$l = 1$	$l = 2$	$l = 10$	$l = 20$
Pseudospectral method	0.088969	0.049719	0.081351	0.080780	0.080755
Direct integration method	0.089669	0.048912	0.081545	0.080502	0.080697
WKB approximation				0.080763	0.080750

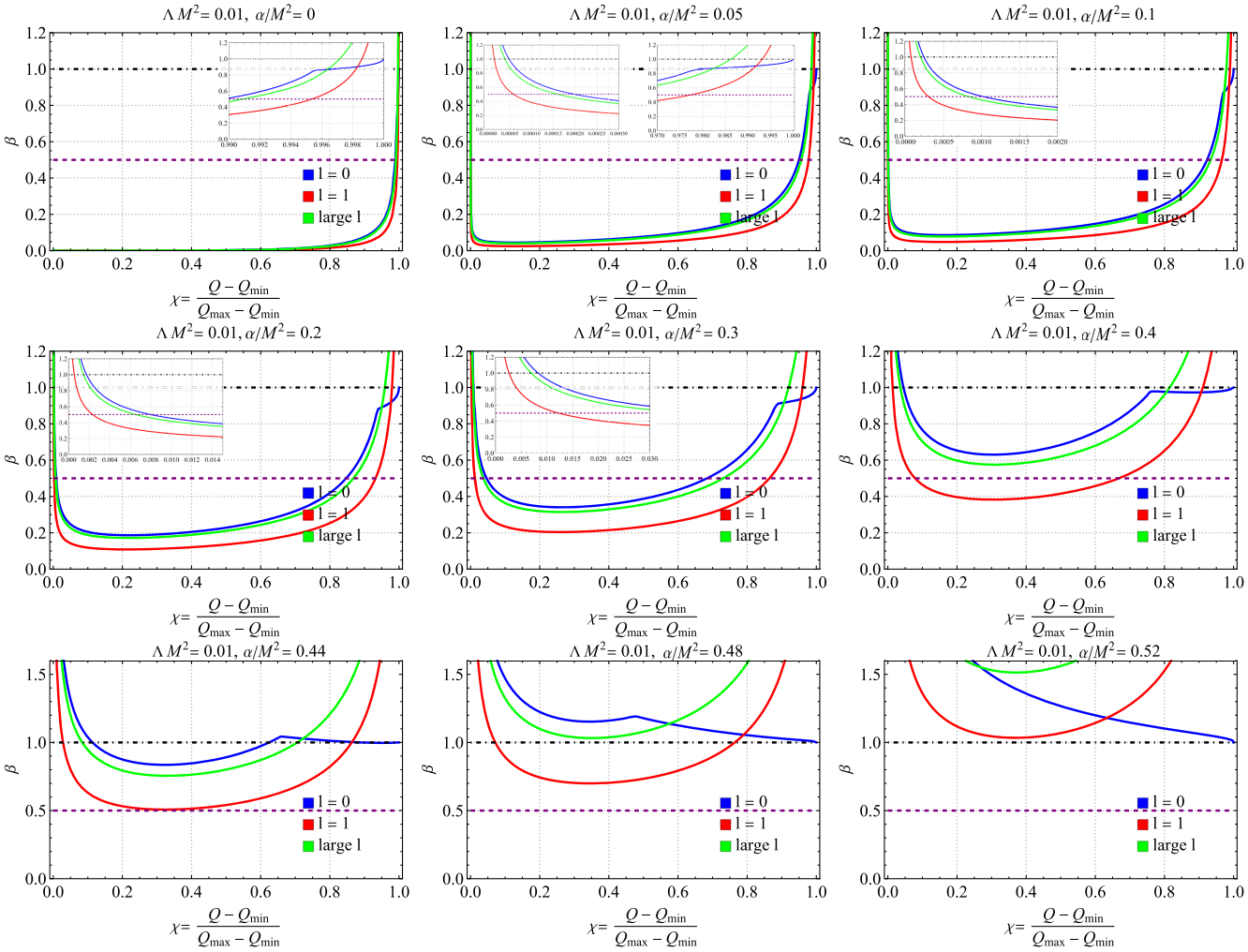

FIG. 4. For $\Lambda M^2 = 0.01$, the figure illustrates the lowest-lying QNMs characterized by $\beta = -\mathrm{Im}(\omega)/\kappa_-$ across different values of α/M^2, with respect to the black-hole charge ratio $\chi = (Q - Q_{\min})/(Q_{\max} - Q_{\min})$ for a constant l. The critical charge ratio for SCC is represented by horizontal dashed lines at $\beta = 1/2$ and $\beta = 1$.

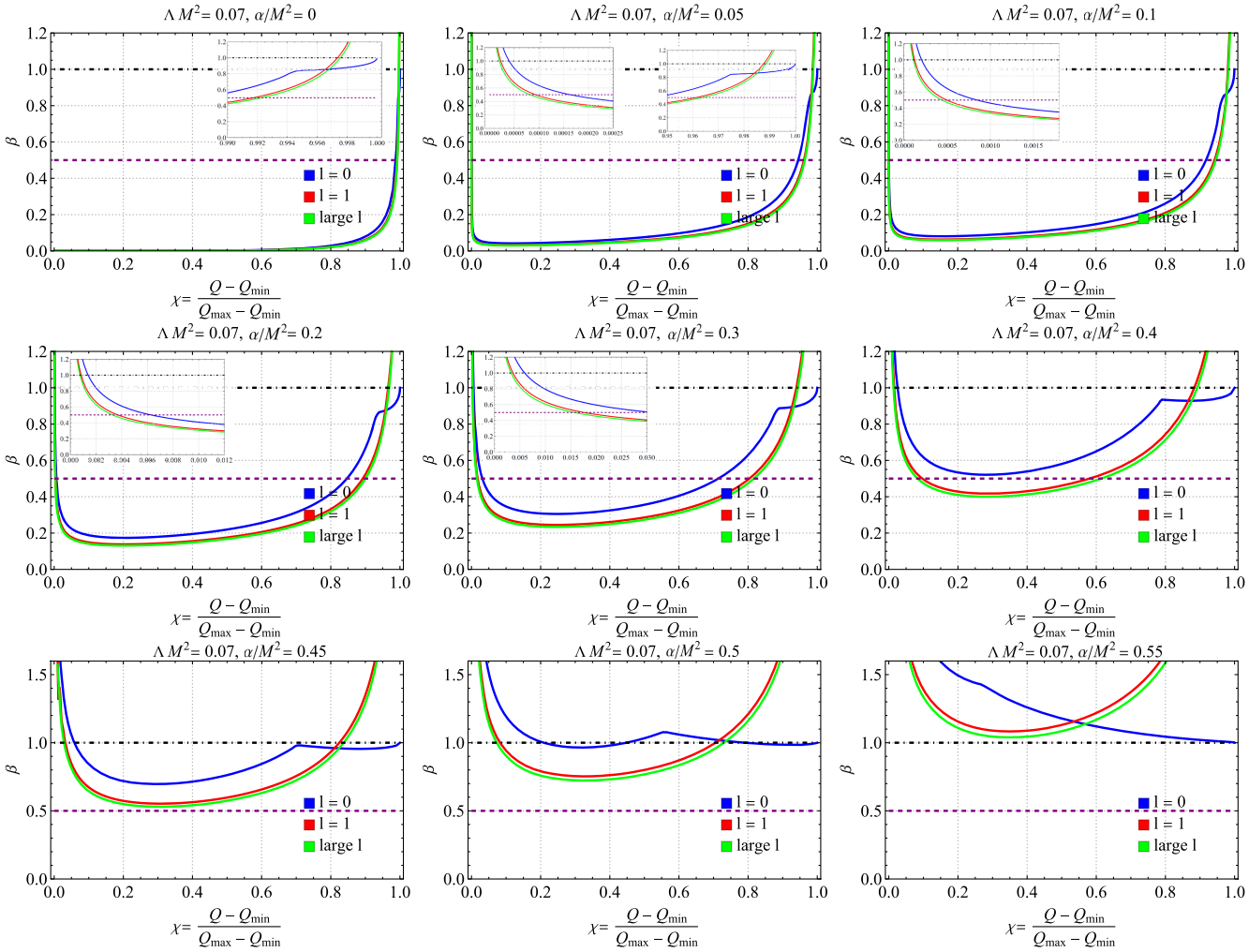

FIG. 5. For $\Lambda M^2 = 0.07$, the figure illustrates the lowest-lying QNMs characterized by $\beta = -\mathrm{Im}(\omega)/\kappa_-$ across different values of α/M^2, with respect to the black-hole charge ratio $\chi = (Q - Q_{\min})/(Q_{\max} - Q_{\min})$ for a constant l. The critical charge ratio for SCC is represented by horizontal dashed lines at $\beta = 1/2$ and $\beta = 1$.

RNdS-like black holes with massless scalar field perturbations, an increase in the Euler-Heisenberg parameter α/M^2 results in instances where the lowest-lying QNMs' β exceeds 1, leading to a violation of the C^2 version of the SCC. Notably, when α/M^2 reaches sufficiently large values, all EHdS black hole solutions contravene the C^2 version of the SCC.

Finally, we explore the impact of the Euler-Heisenberg parameter α/M^2 on the validity of the SCC, particularly analyzing its influence on the validation region of the Christodoulou version of the SCC concerning the charge ratio χ. In Fig. 6, with $\Lambda M^2 = 0.01$, 0.04, and 0.07 held constant, we map the distribution of the lowest-lying QNMs' β within the $\alpha/M^2 - \chi$ parameter space. The shaded pink region denotes where $\beta < 1/2$, presenting the validation region of the Christodoulou version of the SCC, while the blank area represents $\beta > 1/2$, showing the violation region of the SCC. It is apparent from the figures that as α/M^2 increases, the width of the SCC validation interval in χ decreases, suggesting a greater likelihood of SCC violation with higher Euler-Heisenberg parameter values. Furthermore, it is not hard to see that beyond a critical threshold of α/M^2, all black hole solutions violate the SCC.

V. NONMINIMALLY COUPLED SCALAR FIELD PERTURBATION

In this paper, we primarily consider the massless scalar field perturbation. It has been found that the SCC in RNdS black holes can be restored when the theories include perturbations of nonminimally coupled scalar

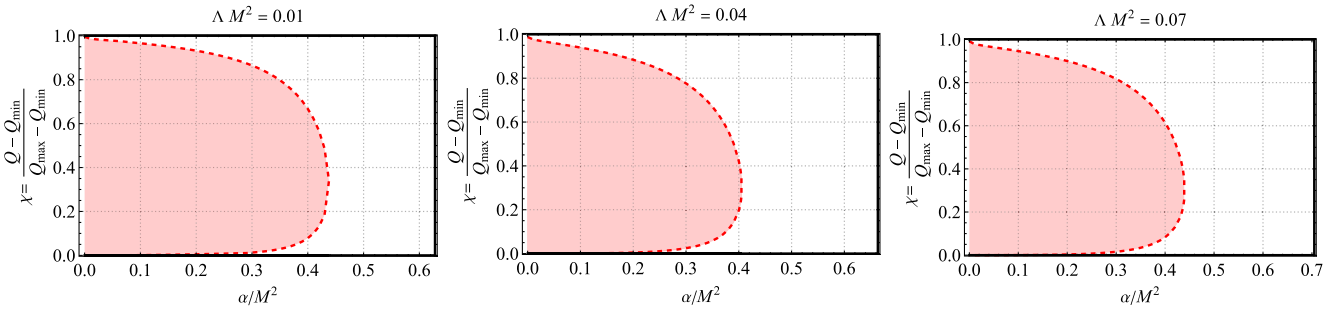

FIG. 6. When $\Lambda M^2 = 0.01$, 0.04, and 0.07, the plots illustrate the distribution of the lowest-lying QNM β in the parameter space of α/M^2 and χ. The pink region represents the area where $\beta < 1/2$, indicating the validation region of the Christodoulou version of the SCC, while the blank region indicates where $\beta > 1/2$, corresponding to the violation region of the SCC.

fields [52,53]. In this section, we aim to extend our research to cases where the scalar field nonminimally couples to gravitational or electromagnetic invariants. As an example, we consider the case where the scalar field is coupled to the electromagnetic invariant, as in [53], where the field equation for this scalar field perturbation is given by

$$\nabla_a \nabla^a \Psi - \frac{b}{2} F_{ab} F^{ab} \Psi = 0, \tag{32}$$

in which b is a coupling constant. Here, $(b/2)F_{ab}F^{ab}$ can be regarded as the effective mass term of the scalar field. Using the same decomposition (16), we obtain

$$\frac{d^2\psi(r)}{dr_*^2} + [\omega^2 - V(r)]\psi(r) = 0, \tag{33}$$

with the effective potential:

$$V(r) = \frac{f(r)}{r^2}\left[l(l+1) + \frac{2M}{r} - \frac{2Q^2}{r^2} - \frac{2\Lambda r^2}{3} + \frac{3\alpha Q^4}{10 r^6} - \frac{bQ^2}{r^2}\right]. \tag{34}$$

Following similar discussions as in Sec. III and Ref. [53], the condition for the validity of the SCC is that there exists at least one QNM satisfying $\beta \leq 1/2$.

For RNdS black holes, corresponding to the case of $\alpha = 0$, it has been shown in Ref. [53] that the SCC can be restored when the coupling constant b exceeds a critical value b_{crit}. Next, we use numerical calculations to explore whether a similar situation can occur in EHdS black holes, specifically whether the SCC violations of the first and second types found earlier in the massless scalar field case can be salvaged when the coupling constant b is sufficiently large. In Fig. 7, we present the numerical results of the lowest-lying mode β for different coupling constants b when $l = 0$, $\Lambda M^2 = 0.01$, and $\alpha/M^2 = 0.2$ (left panel),

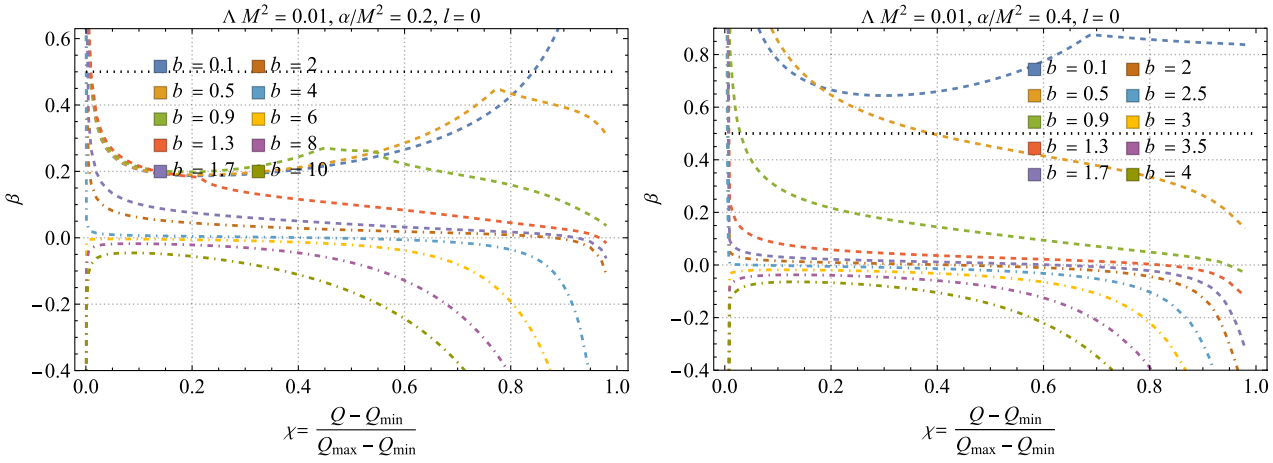

FIG. 7. For $\Lambda M^2 = 0.01$ and $\alpha/M^2 = 0.2$ (left panel), (0.4) (right panel), the figure illustrates the lowest-lying QNMs of $l = 0$ characterized by β across different values of the coupling constant b, with respect to the black hole charge ratio $\chi = (Q - Q_{\text{min}})/(Q_{\text{max}} - Q_{\text{min}})$ for a constant l. The critical charge ratio for SCC is represented by horizontal dotted lines at $\beta = 1/2$.

(0.4) (right panel). As shown in these figures, for a given α/M^2, as long as the coupling constant b is sufficiently large, the lowest-lying modes of QNMs for all charged black holes at $l = 0$ satisfy $\beta < 1/2$, thereby restoring the SCC.

This result is quite easy to understand. By considering the nonminimal coupling between the scalar field and the electromagnetic invariant, the effective mass term of the scalar field becomes negative. When the coupling constant b is sufficiently large, this term induces tachyonic instability. This tachyonic instability is reflected in the QNMs as low-lying modes with $-\mathrm{Im}\omega < 0$. Given that the low-lying modes of QNMs generally vary continuously, it is easy to imagine that when b is large enough, the low-lying modes of QNMs for all black holes will satisfy $\beta < 1/2$, thus validating the SCC.

Additionally, it is worth mentioning that in the case of $-\mathrm{Im}\omega < 0$, due to tachyonic instability, the EHdS black hole undergoes spontaneous scalarization and becomes a scalarized black hole [75–81]. Fortunately, recent literature has demonstrated that any electrodynamic black holes with scalar hair lack a Cauchy horizon, thereby automatically satisfying the requirements of the SCC [82,83]. Therefore, for the case of $-\mathrm{Im}\omega < 0$, the SCC is also automatically validated. Thus, for the scenario we consider, there always exists a sufficiently large nonminimal coupling constant b such that the EHdS black hole satisfies the SCC. Given the aforementioned reasons, it is easy to believe that when the scalar field nonminimally couples to geometric invariants, such as the Gauss-Bonnet term, sufficiently strong nonminimal coupling effects can also restore the SCC.

VI. CONCLUSION

This study focuses on the SCC within the Euler-Heisenberg-dS black holes, aiming to explore the impact of quantum electrodynamical corrections to the Maxwell-Lorentz theory on spacetime causality. With the emergence of Euler-Heisenberg corrections, Euler-Heisenberg-dS black holes exhibit a complex horizon structure, leading to the occurrence of two types of extremal conditions. Specifically, EHdS black holes present four horizons and two types of extremal conditions. The first type resembles the RNdS spacetime, involving coinciding Cauchy and event horizons, while the second type involves the coincidence of the innermost and Cauchy horizons.

We investigate the Cauchy horizon stability in Euler-Heisenberg-dS black holes under the influence of a massless scalar field perturbation. Through numerical calculations of lowest-lying QNMs, we discover that the violation of the SCC not only occurs near the commonly observed first-type extremal solutions but also manifests in the vicinity of second-type extremal black holes. This marks the first instance of SCC violation extending to another region within the classical framework. Additionally, we observe that with an increase in the Euler-Heisenberg parameter, the validation region of the charge ratio shrinks, and beyond a critical value of α/M^2, all black hole solutions violate SCC. These findings suggest an increased likelihood of SCC violation with higher values of the reduced Euler-Heisenberg parameter α/M^2, which implies that the greater the impact of quantum electrodynamical vacuum corrections on the external region of the black hole, the more easily the SCC is violated. Furthermore, when α/M^2 is sufficiently large, violations occur not only for the Christodoulou version but also for the C^2 version of the SCC. This represents the C^2 version SCC violation observed under massless scalar field perturbations, which marks the first instance of C^2 version SCC violation found under massless scalar field perturbations.

Furthermore, our research extended to cases where the scalar field nonminimally couples to gravitational or electromagnetic invariants. We found that for sufficiently large coupling constants b, the lowest-lying modes of QNMs for all charged black holes at $l = 0$ satisfy $\beta < 1/2$, thereby restoring the SCC. This result can also be understood from the tachyonic instability induced when b is large enough. Similarly, we believe that sufficiently strong nonminimal coupling effects to geometric invariants (such as the Gauss-Bonnet term) can also restore the SCC. Considering that the paper mainly focuses on the impact of minimally coupled scalar perturbations on the SCC and that a comprehensive discussion of the violation interval for nonminimal cases requires substantial computational effort, we do not discuss these nonminimal cases in detail in the current paper.

ACKNOWLEDGMENTS

This work is supported by the starting funding of Suzhou University of Science and Technology with Grant No. 332114702, Natural Science Foundation of Jiangsu Province (Grant No. BK20220633), and National Natural Science Foundation of China (Grant No. 12204341).

[1] R. Penrose, Riv. Nuovo Cimento **1**, 252 (1969).
[2] S. Chandrasekhar, Fundam. Theor. Phys. **9**, 5 (1984).
[3] E. Poisson, *A Relativist's Toolkit: The Mathematics of Black-Hole Mechanics* (Cambridge University Press, Cambridge, England, 2009).
[4] J. Sorce and R. M. Wald, Phys. Rev. D **96**, 104014 (2017).
[5] J. An, J. Shan, H. Zhang, and S. Zhao, Phys. Rev. D **97**, 104007 (2018).
[6] B. Ge, Y. Mo, S. Zhao, and J. Zheng, Phys. Lett. B **783**, 440 (2018).
[7] J. Jiang, B. Deng, and Z. Chen, Phys. Rev. D **100**, 066024 (2019).
[8] J. Jiang, X. Liu, and M. Zhang, Phys. Rev. D **100**, 084059 (2019).
[9] J. Jiang, Phys. Lett. B **804**, 135365 (2020).
[10] Y. Qu, J. Tao, and J. Wu, Eur. Phys. J. C **82**, 185 (2022).
[11] X. Y. Wang and J. Jiang, J. High Energy Phys. 05 (2020) 161.
[12] A. Sang and J. Jiang, J. High Energy Phys. 09 (2021) 095.
[13] X. Y. Wang and J. Jiang, Phys. Rev. D **106**, 064050 (2022).
[14] J. Jiang and M. Zhang, Phys. Rev. D **102**, 084033 (2020).
[15] M. Zhang and J. Jiang, Eur. Phys. J. C **80**, 890 (2020).
[16] J. Jiang and M. Zhang, Eur. Phys. J. C **80**, 822 (2020).
[17] J. Jiang, Nucl. Phys. **B984**, 115963 (2022).
[18] D. Christodoulou, Classical Quantum Gravity **16**, A23 (1999).
[19] M. Simpson and R. Penrose, Int. J. Theor. Phys. **7**, 183 (1973).
[20] E. Poisson and W. Israel, Phys. Rev. D **41**, 1796 (1990).
[21] M. Dafermos, Commun. Pure Appl. Math. **58**, 0445 (2005).
[22] M. Dafermos, Commun. Math. Phys. **332**, 729 (2014).
[23] M. Dafermos, I. Rodnianski, and Y. Shlapentokh-Rothman, arXiv:1402.7034.
[24] P. R. Brady, C. M. Chambers, W. Krivan, and P. Laguna, Phys. Rev. D **55**, 7538 (1997).
[25] P. R. Brady, I. G. Moss, and R. C. Myers, Phys. Rev. Lett. **80**, 3432 (1998).
[26] F. Mellor and I. Moss, Phys. Rev. D **41**, 403 (1990).
[27] P. R. Brady, C. M. Chambers, W. G. Laarakkers, and E. Poisson, Phys. Rev. D **60**, 064003 (1999).
[28] C. Molina, D. Giugno, E. Abdalla, and A. Saa, Phys. Rev. D **69**, 104013 (2004).
[29] P. Hintz and A. Vasy, J. Math. Phys. (N.Y.) **58**, 081509 (2017).
[30] V. Cardoso, J. L. Costa, K. Destounis, P. Hintz, and A. Jansen, Phys. Rev. Lett. **120**, 031103 (2018).
[31] Y. Mo, Y. Tian, B. Wang, H. Zhang, and Z. Zhong, Phys. Rev. D **98**, 124025 (2018).
[32] B. Ge, J. Jiang, B. Wang, H. Zhang, and Z. Zhong, J. High Energy Phys. 01 (2019) 123.
[33] X. Liu, S. Van Vooren, H. Zhang, and Z. Zhong, J. High Energy Phys. 10 (2019) 186.
[34] O. J. C. Dias, H. S. Reall, and J. E. Santos, Classical Quantum Gravity **36**, 045005 (2019).
[35] V. Cardoso, J. L. Costa, K. Destounis, P. Hintz, and A. Jansen, Phys. Rev. D **98**, 104007 (2018).
[36] K. Destounis, Phys. Lett. B **795**, 211 (2019).
[37] O. J. C. Dias, H. S. Reall, and J. E. Santos, J. High Energy Phys. 10 (2018) 001.
[38] H. Guo, H. Liu, X. M. Kuang, and B. Wang, Eur. Phys. J. C **79**, 891 (2019).
[39] M. Zhang and J. Jiang, Eur. Phys. J. C **81**, 967 (2021).
[40] X. Y. Nan, J. Tan, and J. Jiang, Eur. Phys. J. C **83**, 424 (2023).
[41] M. Zhang and J. Jiang, Sci. China Phys. Mech. Astron. **66**, 280412 (2023).
[42] H. Liu, Z. Tang, K. Destounis, B. Wang, E. Papantonopoulos, and H. Zhang, J. High Energy Phys. 03 (2019) 187.
[43] M. Rahman, S. Chakraborty, S. SenGupta, and A. A. Sen, J. High Energy Phys. 03 (2019) 178.
[44] O. J. C. Dias, H. S. Reall, and J. E. Santos, J. High Energy Phys. 12 (2019) 097.
[45] K. Destounis, R. D. B. Fontana, and F. C. Mena, Phys. Rev. D **102**, 104037 (2020).
[46] O. J. C. Dias, F. C. Eperon, H. S. Reall, and J. E. Santos, Phys. Rev. D **97**, 104060 (2018).
[47] M. Casals and C. I. S. Marinho, Phys. Rev. D **106**, 044060 (2022).
[48] C. Y. Shao, L. J. Xin, W. Zhang, and C. G. Shao, Phys. Lett. B **835**, 137512 (2022).
[49] M. Dafermos and Y. Shlapentokh-Rothman, Classical Quantum Gravity **35**, 195010 (2018).
[50] R. Luna, M. Zilhão, V. Cardoso, J. L. Costa, and J. Natário, Phys. Rev. D **99**, 064014 (2019).
[51] K. Destounis, R. D. B. Fontana, F. C. Mena, and E. Papantonopoulos, J. High Energy Phys. 10 (2019) 280.
[52] A. Sang and J. Jiang, Phys. Rev. D **105**, 084047 (2022).
[53] J. Jiang and J. Tan, Eur. Phys. J. C **83**, 1132 (2023).
[54] S. Hollands, R. M. Wald, and J. Zahn, Classical Quantum Gravity **37**, 115009 (2020).
[55] G. Mie, Ann. Phys. (Leipzig) **342**, 511 (1912).
[56] M. Born and L. Infeld, Proc. R. Soc. A **144**, 425 (1934).
[57] E. Fradkin and A. Tseytlin, Phys. Lett. **163B**, 123 (1985).
[58] A. Tseytlin, Nucl. Phys. **B276**, 391 (1986); **B291**, 876(E) (1987).
[59] R. G. Leigh, Mod. Phys. Lett. A **04**, 2767 (1989).
[60] L. de Fossé, P. Koerber, and A. Sevrin, Nucl. Phys. **B603**, 413 (2001).
[61] G. W. Gibbons, Nucl. Phys. **B514**, 603 (1998).
[62] H. Yajima and T. Tamaki, Phys. Rev. D **63**, 064007 (2001).
[63] W. Heisenberg and H. Euler, Z. Phys. **98**, 714 (1936).
[64] S. Weinberg, *The Quantum Theory of Fields* (Cambridge University Press, Cambridge, England, 1995).
[65] G. Brodin, M. Marklund, and L. Stenflo, Phys. Rev. Lett. **87**, 171801 (2001).
[66] J. F. Plebanski, *Lectures on Nonlinear Electrodynamics* (Nordita, Copenhagen, 1970).
[67] H. Salazar, A. D. Garcia, and J. Plebanski, J. Math. Phys. (N.Y.) **28**, 2171 (1987).
[68] G. R. Li, S. Guo, and E. W. Liang, Phys. Rev. D **106**, 064011 (2022).
[69] R. A. Konoplya and A. Zhidenko, Rev. Mod. Phys. **83**, 793 (2011).
[70] A. Jansen, Eur. Phys. J. Plus **132**, 546 (2017).
[71] F. S. Miguel, Phys. Rev. D **103**, 064077 (2021).
[72] S. Chandrasekhar and S. L. Detweiler, Proc. R. Soc. A **344**, 441 (1975).

[73] C. Molina, P. Pani, V. Cardoso, and L. Gualtieri, Phys. Rev. D **81**, 124021 (2010).
[74] R. A. Konoplya, Phys. Rev. D **68**, 024018 (2003).
[75] C. A. R. Herdeiro, E. Radu, N. Sanchis-Gual, and J. A. Font, Phys. Rev. Lett. **121**, 101102 (2018).
[76] P. G. S. Fernandes, C. A. R. Herdeiro, A. M. Pombo, E. Radu, and N. Sanchis-Gual, Classical Quantum Gravity **36**, 134002 (2019); **37**, 049501(E) (2020).
[77] Y. S. Myung and D. C. Zou, Phys. Lett. B **790**, 400 (2019).
[78] Y. S. Myung and D. C. Zou, Eur. Phys. J. C **79**, 273 (2019).
[79] M. Zhang and J. Jiang, Phys. Rev. D **107**, 044002 (2023).
[80] Y. S. Myung and D. C. Zou, Eur. Phys. J. C **79**, 641 (2019).
[81] J. Jiang and J. Tan, Eur. Phys. J. C **83**, 290 (2023).
[82] Y. S. An, L. Li, and F. G. Yang, Phys. Rev. D **104**, 024040 (2021).
[83] R. G. Cai, L. Li, and R. Q. Yang, J. High Energy Phys. 03 (2021) 263.